Spatially distributed delay line interferometer based on transmission Bragg scattering

MIGUEL A. PRECIADO,[1,2] ATALLA EL-TAHER[1], KATE SUGDEN[1], AND XUEWEN SHU[3,*]

[1] Aston Institute of Photonic Technologies, Aston University, Birmingham, United Kingdom.
[2] Currently with Optos plc, Dunfermline, United Kingdom.
[3] Wuhan National Laboratory for Optoelectronics, Huazhong University of Science and Technology, Wuhan, China.
* Corresponding author: xshu@hust.edu.cn

A novel approach for a delay line interferometer (DLI) based on transmission Bragg scattering is proposed. We have numerically and experimentally demonstrated for the first time that a Bragg grating can deliver the functionality of an DLI in its transmission mode along a single common interfering optical path, instead of the conventional DLI implementation with two interfering optical paths. As a proof of concept, phase-modulated fiber Bragg gratings have been designed and fabricated, showing the desired functionality in the transmission mode of the Bragg grating. The proposed approach is applicable to any kind of Bragg grating technology, such as volume Bragg gratings, dielectric mirrors, silicon photonics, and other optical waveguide-based Bragg structures.

http://dx.doi.org/10.1364/OL.99.099999

Introduction

Delay line interferometers (DLIs), such as Mach-Zehnder interferometers (MZI), are simple optical devices where the output optical signal is generated by interfering two replicas of the input signal, commonly generated by splitting the input signal in two different optical paths and re-combining them to generate a resulting interference signal. MZIs are used in a wide range of applications, such as the characterization of optical sources: a number of optical signal processing applications: QPSK, DPSK and PSK demodulator and data conversion [1,2]; photonic quantization [3]; chirp and linewidth characteristics of semiconductor lasers [4]; and sensing of various physical and chemical parameters such as temperature, strain, refractive index, displacement curvature, inclination, or vibration [5-12].

Here we report a novel patented [13] implementation of MZIs based on a Bragg grating (BG) operated in transmission mode, named Bragg-MZI or B-MZI, with a fundamentally different physical working principle from conventional MZIs, illustrated in Fig. 1. Instead of having two physically separated optical paths for the interfering signals as showed in Fig. 1(a), in the proposed B-MZI the interfering signals are simultaneously generated and interfered by forward Bragg scattering, in a single common path

along the grating, represented in Fig. 1(b). As a proof of concept, we present the design and fabrication of a B-MZI using an in-fiber implementation, effectively a phase-modulated fiber BG (FBG) in transmission mode, showing the MZI functionality of the device in numerical simulations and experimental measurements. Finally, we conclude with a summary and discussion of the results.
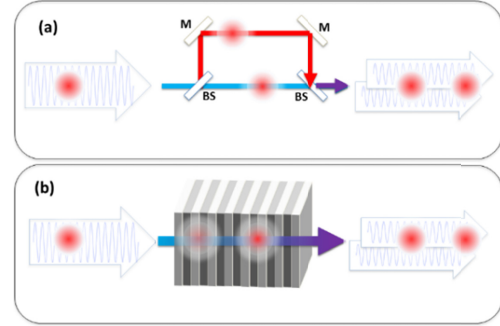

Fig. 1. Comparison of a conventional two-path MZI (free-optics implementation) (a), and a single-path Bragg-MZI (b). BS: Beam Splitter; M: Mirror.

Design and numerical results

An ideal MZI functionally can be expressed in the temporal domain as

$$f_{out}(t) \propto f_{in}(t) + f_{in}(t\text{-}T)\exp(j\phi)$$

where $f_{in}(t)$ and $f_{out}(t)$ are the complex envelopes of the input and output signals respectively, ϕ and T are the relative phase and delay between the interfering components. Equivalently in the frequency domain, we can obtain the spectral transfer function, $H(\omega) = F_{out}(\omega) / F_{in}(\omega)$, as

$$H(\omega) \propto 2\cos(\omega T/2\text{-}\phi/2)\exp(\text{-}j\omega T/2\text{-}j\phi/2)$$

where $F_{out}(\omega)$ and $F_{in}(\omega)$ are the Fourier transforms of $f_{out}(t)$ and $f_{in}(t)$, respectively, ω is the base-band angular pulsation i.e. $\omega = \omega_{opt} - \omega_0$, ω_{opt} is the optical angular pulsation, ω_0 is the central angular frequency of the signals, and $j = (-1)^{1/2}$ is the imaginary unit.

BGs operating in transmission are minimum phase systems [14], therefore it is not possible to achieve a completely arbitrary response using these photonic structures. Fortunately, in our

particular case, the MZI transfer function satisfies the minimum phase condition [15], HT{log|$H(\omega)$|}=$\angle${$H(\omega)$}, where HT denotes the Hilbert transform operator, and $\angle$ denotes the phase operator, which implies that when a BG is designed for delivering the MZI spectral response amplitude in its transmission mode described in Equation (2), the MZI spectral response phase, and therefore the temporal response described in Equation (1), is also automatically obtained.

In principle, there is no theoretical restriction for the kind of BG technology used in the physical implementation of the B-MZI. Here, we have used a fiber Bragg grating (FBG) implementation operating in transmission mode [14,16-25] to demonstrate the proposed approach. Phase-modulated FBGs, initially proposed for virtual Gires-Tournois interferometers in reflection mode [26], have also been proposed and numerically demonstrated as an alternative feasible implementation for some specific spectral responses for pulse shaping in transmission mode [25]. The grating strength is more challenging to accurately control in the fabrication process than the grating period due to the fiber photosensitivity variability, and the non-linear relation between the writing illumination power and the corresponding fiber core refractive index modification. However, in a phase-modulated BG the grating strength remains basically uniform along most of the grating length, while the grating functionality is defined by modulating the grating period, which is much easier to accurately control in the fabrication process in practice.
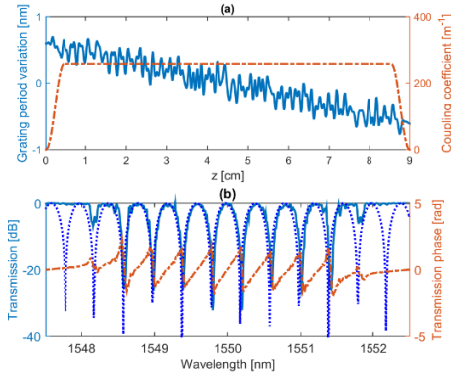

Fig. 2. (a) Grating apodization (red-dash-dotted) and period (blue-solid) obtained from numerical optimization to approach the desired spectral response. (b) Numerically simulated spectral response amplitude of the designed FBG in transmission mode, obtained in amplitude (blue-solid), and phase (red-dash-dotted), and ideal spectral response amplitude (blue-dotted) used as objective in the numerical optimization.

In this design process we have considered the capabilities of our fabrication system. We have defined a grating length of 9 cm with a bandwidth of approximately 4 nm centered at λ_0=1550 nm. Following a numerical optimization process using a similar procedure to that described in [25], we have obtained a grating period function corresponding to the desired spectral function $H(\omega)$, where the MZI parameters have been set to T=20 ps, and ϕ=0. The resulting grating strength and grating period is shown in Fig. 2 (a), and the corresponding data set is accessible in Data File S1 to facilitate the reproducibility of these results to other researchers. As it can be observed in Fig. 2 (b), the numerically simulated spectral response in transmission of the FBG is in good agreement with the ideal response of the MZI.

In order to validate the functionality of the designed B-MZI, we define two input signal examples. The first one with a single pulse to show the basic working principle, and the second one with a test sequence of pulses as an input signal that includes all possible cases of the MZI functionality. Let us define an input signal compose by a single optical pulse $f_{in}(t) = p(t)$ for the first example, where $p(t)$ is the complex envelope function of optical Gaussian pulses of 5 ps full width half maximum (FWHM), with central wavelength $\lambda_0 = 2\pi/\omega_0$=1550 nm. From Eq. (1) we can deduce that the output sequence of the ideal MZI is $f_{out}(t) = \sum_{k=1}^{2} d_k p(t - kT)$, with $d_k \propto \{1,1\}$ (i.e. $d_1 \propto 1$, $d_2 \propto 1$), with an intensity $I_{out}(t) = |f_{out}(t)|^2 \simeq \sum_{k=1}^{2} |d_k|^2 |p(t - kT)|^2$, where we have assumed $p(t-mT)p^*(t-nT) \simeq 0$ for m≠n (negligible pulses overlapping), and the total transmission delay is neglected.

In the second input signal example, we define a test sequence composed of multiple optical pulses to numerically verify the B-MZI functionality. The pulses sequence is defined by $f_{in}(t) = \sum_{k=1}^{5} c_k p(t - kT)$, where c_k={1,0,1,1,-1}. Applying Eq. (1) we can deduce that the output sequence of the ideal MZI is given by: $f_{out}(t) = \sum_{k=1}^{5} d_k p(t - kT)$, where $d_k \propto c_k + c_{k+1}$={1,1,1,2,0,-1}, and with an intensity of $I_{out}(t) = |f_{out}(t)|^2 \simeq \sum_{k=1}^{5} |d_k|^2 |p(t - kT)|^2$, where again we have assumed $p(t-mT)p^*(t-nT) \simeq 0$ for m≠n (negligible pulses overlapping), and the total transmission delay is not taken into account.
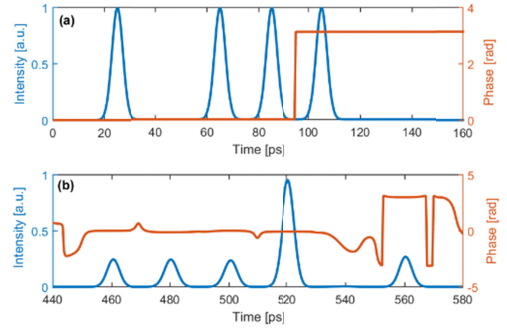

Fig. 3. Numerical simulation results of the designed BG with the input pulses sequence defined above, where the output intensity and phase are in good agreement with the expected $I_{out}(t)$. Visualization 1 shows an animated representation of the temporal evolution the optical intensity spatial distribution inside the Bragg structure, in transmitted and reflected mode, for both the input single pulse and the pulse sequence.

In order to illustrate the physical generation of the interference of the B-MZI in a common interfering path, and to emphasize the difference with conventional two interfering paths MZIs approaches, we have also calculated the optical intensity distribution inside the designed BG as it propagates along the grating by using the numerical method proposed in [27] by Muriel and Carballar. Figure 4 represents the intensity distribution inside the grating for the single incident optical pulse as defined above, for both transmitted and reflected both, showing the temporal and spectral distribution of the optical intensity. From the temporal

distribution of the transmitted mode inside the grating, we can observe how the transmitted pulse is gradually split and recombined in a spatially distributed way into two components as the signal propagates along the common path, without requiring a spatial splitting in different paths at any point. Also, from the spectral analysis of the transmitted signal along the grating represented, we can observe the spatial distribution of the spectral components transmitted through the grating, where the minimum phase condition imposes the desired spectral phase.
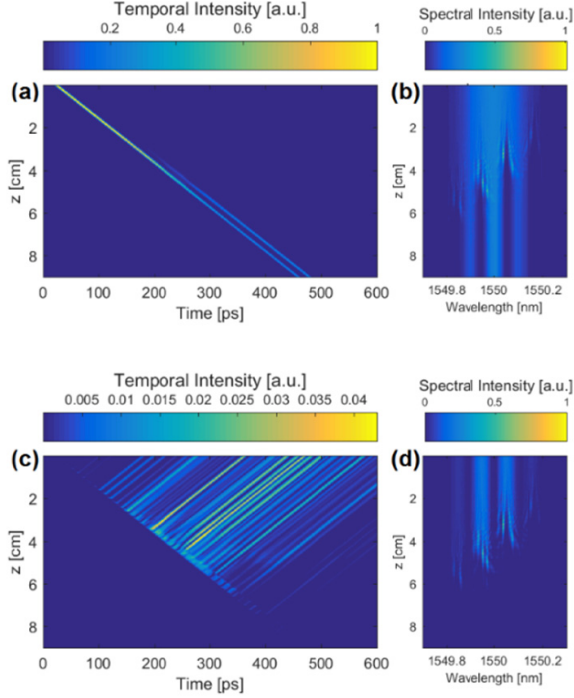

Fig. 4. Spatio-temporal optical intensity distribution inside the FBG for a single Gaussian input pulse example, corresponding to the reflection mode (a), and the transmission mode (c). The spatial distribution of the spectral intensity is represented in subplots (b) and (d) for reflection and transmission modes, respectively.

Experimental demonstration

A phase-modulated FBG has been fabricated with the previously calculated grating strength and period, using a UV laser direct-writing system developed at Aston University, where the grating is created pitch-by-pitch, and the coupling coefficient profile and the varied period are realized by controlling the ON/OFF of an acoustic optical modulator and moving the phase mask/fiber. A hydrogen-loaded photosensitive fiber, later stabilized by annealing at 80℃ for 60 h after the fabrication of the grating, was used in the process. The fabricated FBG has been characterized using a broad spectrum light source as excitation, and measuring the output spectrum of the FBG in transmission, which is shown in Fig. 5(a) compared to the ideal MZI interferometer. The corresponding spectral phase is also showed in Fig. 5(b), which has been numerically recovered from the previous spectral intensity measurement by using the Hilbert transform relations of the transmission spectral response amplitude/phase [14], a method reported as more robust than spectral interferometry in [28]. Although the transmission mode phase response is less sensitive to grating-fabrication errors than in reflection mode [14,30], still the errors in the fabrication process affects as a distortion of the FBG spectral response amplitude and

phase, as observed in Fig. 5 (a) and (b), as described in [29]. A more accurate fabrication process could be needed to reduce this distortion, depending on the application requirements.
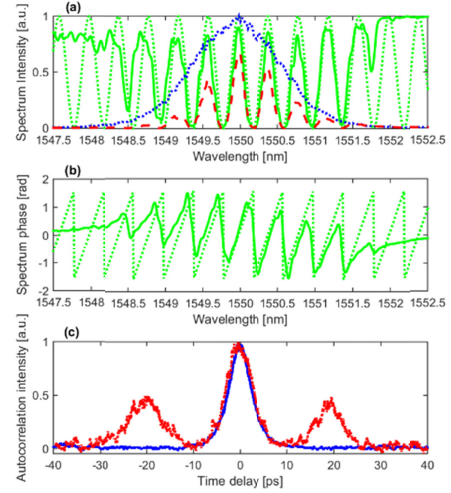

Fig. 5. (a) Spectral response intensity of the ideal MZI (green-dashed), compared to the measured spectral response intensity (green-solid) of the fabricated FBG in transmission when excited with a broad source; spectrum of the pulsed laser source used as an input signal (blue-solid), and the corresponding output of the FBG in transmission mode (red-dashed); (b) Spectral response phase of the ideal MZI (green-dashed) compared to the Hilbert transform recovered spectral response phase of the fabricated FBG (green-solid); (c) auto-correlation trace for input (blue-solid) and output (red-dotted) signals, revealing a double pulse output separated 20 ps (as designed) from a single pulse input.

The response to optical pulses in transmission mode of the fabricated FBG has been characterized by using a pulsed laser based on an Erbium gain based single-walled carbon nanotube (CNT) passively-mode-locked fiber laser as excitation, where the spectrum of these pulsed laser input and the corresponding FBG-MZI output is also showed in Fig. 5(a). The input and output signals has been also characterized in temporal domain by using an intensity auto-correlator, where the autocorrelation of input and output is showed in Fig. 5(c). As it can be observed, the autocorrelation intensity indicates an output signal composed by a double pulse with a relative delay of approximately 20 ps in the output signal, matching the designed MZI functionality.

Regarding the environmental sensitivity/tunability properties of the fabricated FBG-MZI, we have verified that the central Bragg wavelength can be shifted by the application of either temperature or strain variation while the spectral response remains approximately undistorted ([31-33]), where we obtained a spectral shift of 9.81×10^{-3} nm/℃ for temperature, and 1.14×10^{-3} nm/μɛ for strain. Taking into account that a shift in wavelength of 0.8014 nm (free spectral range) corresponds to a variation of 2π in ϕ, we can easily deduce the dependence of ϕ on temperature to be 76.9 mrad/℃, and on strain to be 8.9 mrad/μɛ.

Conclusion and discussion

We have proposed and demonstrated a novel implementation of a MZI based on a Bragg resonant structure in transmission mode, with a fundamental working principle fundamentally different to that of conventional two-interfering paths MZIs. As a proof of concept, an optical fiber implementation of a B-MZI using a phase-

modulated FBG was designed and fabricated. In the numerical simulations we have shown the desired MZI functionality of the designed FBG, and for illustrative purpose the optical intensity distribution inside the Bragg grating has also been calculated, showing how the forward Bragg scattering generates a single common path interference in a distributed way along the Bragg grating.

It is worth noting that here we also report the first experimental demonstration of a phase-modulated FBG for the synthesis of a specific spectral response in transmission mode, which were proposed but only numerically demonstrated in [25] for some pulse shaping applications. It is also important to differentiate the MZI functional block, which performs a general functionality that delivers an output signal depending on the input signal, from pulse shapers, which deliver a much more fixed operation, where a specific desired output waveform is obtained from a usually previously known input waveform.

Sensitivity to environmental changes is typically high in conventional two path based MZIs, where any relative variation of the effective optical paths of the interfering components in the order of a fraction of a wavelength produces a significant variation of the response, making them very suitable for sensing applications of small perturbations. Additionally, for in-fiber implementation of two-paths MZIs, any relative difference in the polarization state in the MZI paths will affect to the performance. In our case, the proposed Bragg-MZI has a common interfering path, leading to a high robustness to environmental changes. With an athermal packaged FBG a thermal sensitivity of < 0.01 nm (*OEquest*, part number 91000223-063), in a temperature range from -5 °C to +70 °C can be obtained, which correspond to maximum MZI relative phase variation ϕ <78.4 mrad over a temperature range of 75 °C. Due to its robustness and we envision its main use for the implementation of DLI functionality in all optical signal processing, with less relevance in optical sensing applications.

Compared to other DLIs approaches, this approach only provides one signal output, which indeed could be a demerit in some cases. However, it also offers other very interesting possibilities, such as the possibility of passive athermal packaging without any power consumption, instead of active temperature control used in other waveguide type MZIs. It also has a clear potential in extremely inexpensive manufacturing procedure (e.g. by a using custom phase mask in the Bragg writing), Moreover, the combined resonant optical processing together to the operation in transmission mode lead to a device that has the unique capability of performing a DLI operation in a controlled limited spectral band, leaving the rest of the optical spectral bands essentially undistorted. And finally, fiber gratings have a natural compatibility with optical fibers, being able to directly process optical signals without the need for coupling/re-coupling alignments required by bulk-optics or chip based devices, thus provide a low-loss, stable, cost-effective and ultra-fast solution for optical signal processing.

In conclusion, we introduce here a new paradigm for DLIs, based on Bragg structures and interfering transmission modes in a common optical path, which can be applied to any kind of Bragg grating technology (such as volume Bragg gratings, dielectric mirrors, silicon photonics, or other optical waveguide technologies based Bragg structures) beyond the demonstrated in-fiber implementation here.

Funding

References

1. R. Kou, H. Nishi, T. Tsuchizawa, H. Fukuda, H. Shinojima, and K. Yamada, Opt. Express 20, 11037-11045 (2012).
2. Z. Zhang, Y. Yu, and X. Zhang, Opt. Express 19, 12427 (2011).
3. H. Chi, Z. Li, X. Zhang, S. Zheng, X. Jin, and J. Yao, Opt. Lett. 36, 1629 (2011).
4. N. Satyan, A. Vasilyev, G. Rakuljic, V. Leyva, and A. Yariv, Opt. Express 17, 15991 (2009).
5. L. Xu, Y. Li, and B. Li, Appl. Phys. Lett. 101, 153510 (2012).
6. Y. Xu, Ping Lu, Zengguang Qin, Jeremie Harris, Farhana Baset, Ping Lu, Vedula Ravi Bhardwaj, and Xiaoyi Bao, Opt. Express 21, 3031 (2013)
7. H. F. Martins, J. Bierlichc, K.Wondraczekc, S. Ungerc, J. Kobelkec, K. Schusterc, M. B. Marquesa,b, M. Gonzalez-Herraezd, O. Frazãoa, OFS2014 23rd International Conference on Optical Fiber Sensors. International Society for Optics and Photonics, 2014.
8. P. Lu and Q. Chen, Opt. Lett. 36, 268 (2011).
9. Z. Tian, S. S.-H. Yam, J. Barnes, W. Bock, P. Greig, J. M. Fraser, H.-P. Loock, and R. D. Oleschuk, IEEE Photon. Technol. Lett. 20, 626 (2008).
10. J. Chen, J. Zhou, and X. Yuan, IEEE Photon. Technol. Lett. 26, 837 (2014).
11. T. Wei, X. Lan, and H. Xiao, IEEE Photon. Technol. Lett. 21, 669 (2009).
12. C. R. Liao, Y. Wang, D. N. Wang, and M. Yang, Fourth European Workshop on Optical Fibre Sensors. International Society for Optics and Photonics (2010).
13. X Shu, MA Preciado, US Patent 20160109657.
14. J. Skaar, J. Opt. Soc. Am. A 18, 557 (2001).
15. F.W. King, *Hilbert Transforms* (Cambridge University Press, 2009).
16. N. M. Litchinitser, B. J. Eggleton, and D. B. Patterson, J. Lightwave Technol. 15, 1303 (1997)
17. M. A. Preciado and M. A. Muriel, Opt. Lett. 33, 2458 (2008)
18. L. M. Rivas, S. Boudreau, Y. Park, R. Slavík, S. LaRochelle, A. Carballar, and J. Azaña, Opt. Lett. 34, 1792 (2009).
19. N. Q. Ngo, Opt. Lett. 32, 3020 (2007)
20. M. H. Asghari and J. Azaña, Opt. Express 16, 11459(2008).
21. M. A. Preciado and M. A. Muriel, Opt. Lett. 34, 752 (2009).
22. M. Fernández-Ruiz, M. Li, M. Dastmalchi, A. Carballar, S. LaRochelle, and J. Azaña, Opt. Lett. 38, 1247-1249 (2013).
23. M. Burla, M. Li, L. Cortés, X. Wang, M. Fernández-Ruiz, L. Chrostowski, and J. Azaña, Opt. Lett. 39, 6241-6244 (2014).
24. M. Fernández-Ruiz, L. Wang, A. Carballar, M. Burla, J. Azaña, and S. LaRochelle, Opt. Lett. 40, 41-44 (2015).
25. M. Preciado, X. Shu, and K. Sugden, Opt. Lett. 38, 70-72 (2013).
26. X. Shu, K. Sugden, and K. Byron, Opt. Lett. 28, 881-883 (2003)
27. M. A. Muriel and A. Carballar, IEEE Photon.Technol. Lett., vol. 9, no. 7, p. 955, Jul. 1997.
28. M. Dicaire, J. Upham, I. De Leon, S. A. Schulz, and R. W. Boyd, J. Opt. Soc. Am. B 31, 1006-1010 (2014)
29. R. Feced, M. N. Zervas, J. Lightwave Technol. 18, 90-101 (2000).
30. K. Hinton, J. Lightwave Technol. 16, 2336- (1998)
31. K.-M. Feng, J.-X. Cai, V. Grubsky, D. S. Starodubov, M. I. Hayee, S. Lee, X. Jiang, A. E. Willner, and J. Feinberg, IEEE Photon. Technol. Lett., vol. 11, pp. 373–375, 1999.
32. C. S. Goh, S. Y. Set, and K. Kikuchi, IEEE Photon. Technol. Lett., vol. 14, no. 9, pp. 1306–1308, Sep. 2002
33. J. Lauzon, S. Thibault, M. J, and F. Ouellette, Opt. Lett., vol. 19, pp. 2027–2029, 1994.
34. G. Ducournau, O. Latry, and M. Ketata, Syst., Cybernet. Inf., vol. 4, no. 4, pp. 78–89, 2006.

References (Full)

1. R. Kou, H. Nishi, T. Tsuchizawa, H. Fukuda, H. Shinojima, and K. Yamada, "Single silicon wire waveguide based delay line interferometer for DPSK demodulation," Opt. Express 20, 11037-11045 (2012).

2. Z. Zhang, Y. Yu, and X. Zhang, "Simultaneous all-optical demodulation and format conversion for multi-channel (CS)RZ-DPSK signals," Opt. Express 19, 12427 (2011).

3. H. Chi, Z. Li, X. Zhang, S. Zheng, X. Jin, and J. Yao, "Proposal for photonic quantization with differential encoding using a phase modulator and delay-line interferometers," Opt. Lett. 36, 1629 (2011).

4. N. Satyan, A. Vasilyev, G. Rakuljic, V. Leyva, and A. Yariv, "Precise control of broadband frequency chirps using optoelectronic feedback," Opt. Express 17, 15991 (2009).

5. L. Xu, Y. Li, and B. Li, "Nonadiabatic fiber taper-based Mach-Zehnder interferometer for refractive index sensing," Appl. Phys. Lett. 101, 153510 (2012).

6. Y. Xu, Ping Lu, Zengguang Qin, Jeremie Harris, Farhana Baset, Ping Lu, Vedula Ravi Bhardwaj, and Xiaoyi Bao, "Vibration sensing using a tapered bend-insensitive fiber based Mach-Zehnder interferometer," Opt. Express 21, 3031 (2013)

7. H. F. Martins, J. Bierlichc, K.Wondraczekc, S. Ungerc, J. Kobelkec, K. Schusterc, M. B. Marquesa,b, M. Gonzalez-Herraezd, O. Frazãoa, "In-line Mach-Zehnder interferometer based on a dissimilar-doping dual-core fiber for high sensitivity strain and temperature sensing," OFS2014 23rd International Conference on Optical Fiber Sensors. International Society for Optics and Photonics, 2014.

8. P. Lu and Q. Chen, "Femtosecond laser microfabricated fiber Mach–Zehnder interferometer for sensing applications," Opt. Lett. 36, 268 (2011).

9. Z. Tian, S. S.-H. Yam, J. Barnes, W. Bock, P. Greig, J. M. Fraser, H.-P. Loock, and R. D. Oleschuk, "Refractive Index Sensing With Mach–Zehnder Interferometer Based on Concatenating Two Single-Mode Fiber Tapers," IEEE Photon. Technol. Lett. 20, 626 (2008).

10. J. Chen, J. Zhou, and X. Yuan, "M–Z Interferometer Constructed by Two S-Bend Fibers for Displacement and Force Measurements," IEEE Photon. Technol. Lett. 26, 837 (2014).

11. T. Wei, X. Lan, and H. Xiao, "Fiber Inline Core–Cladding-Mode Mach–Zehnder Interferometer Fabricated by Two-Point CO2 Laser Irradiations," IEEE Photon. Technol. Lett. 21, 669 (2009).

12. C. R. Liao, Y. Wang, D. N. Wang, and M. Yang, "Multi-parameter sensor using fiber In-line MZ Interferometer Embedded in Fiber Bragg Grating," Fourth European Workshop on Optical Fibre Sensors. International Society for Optics and Photonics (2010).

13. X Shu, MA Preciado, "Single fiber Bragg grating as delay line interferometer," US Patent 20160109657.

14. J. Skaar, "Synthesis of fiber Bragg gratings for use in transmission," J. Opt. Soc. Am. A 18, 557 (2001).

15. F.W. King, *Hilbert Transforms* (Cambridge University Press, 2009).

16. N. M. Litchinitser, B. J. Eggleton, and D. B. Patterson, "Experimental demonstration of ultrafast all-fiber high-order photonic temporal differentiators," J. Lightwave Technol. 15, 1303 (1997)

17. M. A. Preciado and M. A. Muriel, "Design of an ultrafast all-optical differentiator based on a fiber Bragg grating in transmission," Opt. Lett. 33, 2458 (2008)

18. L. M. Rivas, S. Boudreau, Y. Park, R. Slavík, S. LaRochelle, A. Carballar, and J. Azaña, "Experimental demonstration of ultrafast all-fiber high-order photonic temporal differentiators," Opt. Lett. 34, 1792 (2009).

19. N. Q. Ngo, "Design of an optical temporal integrator based on a phase-shifted fiber Bragg grating in transmission," Opt. Lett. 32, 3020 (2007)

20. M. H. Asghari and J. Azaña, "Design of all-optical high-order temporal integrators based on multiple-phase-shifted Bragg gratings," Opt. Express 16, 11459(2008).

21. M. A. Preciado and M. A. Muriel, "Flat-top pulse generation based on a fiber Bragg grating in transmission," Opt. Lett. 34, 752 (2009).

22. M. Fernández-Ruiz, M. Li, M. Dastmalchi, A. Carballar, S. LaRochelle, and J. Azaña, "Picosecond optical signal processing based on transmissive fiber Bragg gratings," Opt. Lett. 38, 1247-1249 (2013).

23. M. Burla, M. Li, L. Cortés, X. Wang, M. Fernández-Ruiz, L. Chrostowski, and J. Azaña, "Terahertz-bandwidth photonic fractional Hilbert transformer based on a phase-shifted waveguide Bragg grating on silicon," Opt. Lett. 39, 6241-6244 (2014).

24. M. Fernández-Ruiz, L. Wang, A. Carballar, M. Burla, J. Azaña, and S. LaRochelle, "THz-bandwidth photonic Hilbert transformers based on fiber Bragg gratings in transmission," Opt. Lett. 40, 41-44 (2015).

25. M. Preciado, X. Shu, and K. Sugden, "Proposal and design of phase-modulated fiber gratings in transmission for pulse shaping," Opt. Lett. 38, 70-72 (2013).

26. X. Shu, K. Sugden, and K. Byron, "Bragg-grating-based all-fiber distributed Gires–Tournois etalons," Opt. Lett. 28, 881-883 (2003)

27. M. A. Muriel and A. Carballar, "Internal field distributions in fiber bragg gratings," IEEE Photon.Technol. Lett., vol. 9, no. 7, p. 955, Jul. 1997.

28. M. Dicaire, J. Upham, I. De Leon, S. A. Schulz, and R. W. Boyd, "Group delay measurement of fiber Bragg grating resonances in transmission: Fourier transform interferometry versus Hilbert transform," J. Opt. Soc. Am. B 31, 1006-1010 (2014)

29. R. Feced, M. N. Zervas, "Effect of random phase and amplitude errors in optical fiber gratings," J. Lightwave Technol. 18, 90-101 (2000).

30. K. Hinton, "Dispersion Compensation Using Apodized Bragg Fiber Gratings in Transmission," J. Lightwave Technol. 16, 2336- (1998)

31. K.-M. Feng, J.-X. Cai, V. Grubsky, D. S. Starodubov, M. I. Hayee, S. Lee, X. Jiang, A. E. Willner, and J. Feinberg, "Dynamic dispersion compensation in a 10 Gbit/s optical system using a voltage controlled tuned nonlinearly chirped fiber Bragg grating," IEEE Photon. Technol. Lett., vol. 11, pp. 373–375, 1999.

32. C. S. Goh, S. Y. Set, and K. Kikuchi, "Widely tunable optical filters based on fiber Bragg gratings," IEEE Photon. Technol. Lett., vol. 14, no. 9, pp. 1306–1308, Sep. 2002

33. J. Lauzon, S. Thibault, M. J, and F. Ouellette, "Implementation and characterization of fiber Bragg gratings linearly chirped by temperature gradient," Opt. Lett., vol. 19, pp. 2027–2029, 1994.

34. G. Ducournau, O. Latry, and M. Ketata, "The all-fiber MZI structure for optical DPSK demodulation and optical PSBT encoding," Syst., Cybernet. Inf., vol. 4, no. 4, pp. 78–89, 2006.